Available online at www.sciencedirect.com
ScienceDirect
Bioelectrochemistry 70 (2007) 380–386
Bioelectrochemistry
www.elsevier.com/locate/bioelechem

Ion channels of N-terminally linked alamethicin dimers: Enhancement of cation-selectivity by substitution of Glu for Gln at position 7

Takashi Okazaki [a], Yasuo Nagaoka [b], Koji Asami [c,*]

[a] *Graduate School of Science, Osaka University, Toyonaka 560-0043, Japan, and Research Institute for Cell Engineering, National Institute of Advanced Industrial Science and Technology (AIST), Ikeda 563-8577, Japan*
[b] *Department of Biotechnology, Kansai University, Suita, Osaka 564-8680, Japan*
[c] *Institute for Chemical Research, Kyoto University, Uji, Kyoto 611-0011, Japan*

Received 30 March 2006; received in revised form 8 May 2006; accepted 16 May 2006
Available online 23 May 2006

Abstract

Alamethicin forms voltage-gated ion channels that have moderate cation-selectivity. The enhancement of the cation-selectivity by introducing negatively charged residues at positions 7 and 18 has been studied using the tethered homodimers of alamethicin with Q7 and E18 (di-alm-Q7E18) and its analog with E7 and Q18 (di-alm-E7Q18). In the dimeric peptides, monomer peptides are linked at the N-termini by a disulfide bond. Both the peptides formed long lasting ion channels at *cis*-positive voltages when added to the *cis*-side membrane. Their long open duration enabled us to obtain current–voltage (I–V_m) relations and reversal potentials at the single-channel level by applying a voltage ramp during the channel opening. The reversal potentials measured in asymmetric KCl solutions indicated that ionized E7 provided strong cation-selectivity, whereas ionized E18 little influenced the charge selectivity. This was also the case for the macroscopic charge selectivity determined from the reversal potentials obtained by the macroscopic I–V_m measurements. The results are accounted for by stronger electrostatic interactions between permeant ions and negatively charged residues at the narrowest part of the pore than at the pore mouth.

Keywords: Alamethicin; Ion channel; Planar BLM; Charge selectivity; Reversal potential

1. Introduction

Alamethicin is a well-studied channel forming peptide of 20 residues (Fig. 1), which forms voltage-gated ion channels in lipid bilayers [1–6]. The multi-conductance behavior in the single-channel recordings is interpreted in terms of the helix-bundle model [6–8], which is a basic design for the pore region of intrinsic ion channels. Because of the structural resemblance to intrinsic ion channels as well as the simple sequence, alamethicin has provided a good model channel to study structure–function relationships (for reviews, see Refs. [9–13]). Hence, effects of structural modifications in alamethicin on the channel properties have been extensively studied, and various channel forming peptides based on alamethicin have been designed to mimic the function of intrinsic ion channels, such as ion-selectivity, gating and sensing [14–30]. This study has been performed along the same line and is concerned with the modification of the ion-selectivity of alamethicin channels.

Ion-selectivity of ion channels is commonly evaluated in terms of the ratio of permeability coefficient determined from the reversal potential (or the diffusion potential) evoked in the presence of a salt concentration gradient. It is, however, difficult with alamethicin channels to measure reversal potentials in either single- or multi-channel measurements because of their voltage-dependent channel formation, i.e., the channels formed at a voltage, say 100 mV, close before reaching the reversal potential when the voltage decreases. Alternatively, we often use the ratio of single-channel conductance measured in symmetric solutions of various kinds of salts [26, 31] and in the presence of a salt concentration gradient [32]. Unfortunately, the conductance ratio is not necessarily consistent with the ratio of permeability coefficient determined from the reversal potential [26].

Recently, use of tethered alamethicin made it possible to measure the reversal potentials at the single-channel level.

* Corresponding author. Tel.: +81 774 38 3081; fax: +81 774 38 3084.
E-mail address: asami@e.kuicr.kyoto-u.ac.jp (K. Asami).

1567-5394/$ - see front matter © 2006 Elsevier B.V. All rights reserved.
doi:10.1016/j.bioelechem.2006.05.005

Alamethicin and its analog

alm-Q7E18 (alamethicin Rf30): X7=Q, X18=E
alm-E7Q18: X7=E, X18=Q

Ac-U-P-U-A-U-A-X7-U-V-G-L-U-P-V-U-U-X18-Q-Pheol

Covalently-linked dimers

di-alm-Q7E18: X7=Q, X18=E
di-alm-E7Q18: X7=E, X18=Q

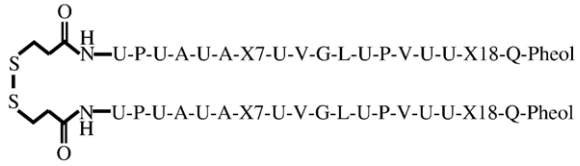

Fig. 1. Amino acid sequences of alamethicin Rf 30 (alm-Q7E18), its analog with E7 and Q18 (alm-E7Q18) and their dimers (di-alm-Q7E18 and di-alm-E7Q18) in which monomers are linked at their N-termini by a disulfide bond. U, α-aminoisobutyric acid; Pheol, phenylalaninol; Ac, acetyl.

Tethering stabilizes specific conductance states to increase the duration of open channels and reduce the rate of channel closure [22–26,30], thereby enabling us to obtain the entire current–voltage (I–V_m) curves for the single channels by applying a fast voltage ramp during the open state [24,25,30]. Using this technique, Starostin et al. [26] studied the ion-selectivity of the single channels formed by covalently linked dimers of alamethicin analogs, and clearly demonstrated that the substitution of Lys (K) for Gln18 (Q18) converted cation-selective channels into anion-selective ones at pH 6.8; the permeability ratio of K^+ to Cl^- (P_K/P_{Cl}) for channels with octameric helices was 2.1 for the peptide with Q18 and 0.56 for the peptide with K18. Furthermore, the ion-selectivity for the peptide with K18 depended on the pH of the bathing solution, i.e., $P_K/P_{Cl}=0.25$ at pH<7, $P_K/P_{Cl}\approx 1$ at pH 7–11 and $P_K/P_{Cl}=4$ at pH>11 [28].

In macroscopic (or multi-channel) measurements, some of the channels can survive at lower voltages around the reversal potential when the voltage is decreased at a relatively high sweep rate. The probability of remaining open channels is a function of the voltage sweep rate, the lifetime of channels and the number of peptides in the membrane. For alamethicin channels with a relatively short lifetime, a relatively high peptide concentration is required to increase the probability, but it also makes the membrane unstable. Measurement of the reversal potential, therefore, is not easy task for alamethicin channels. Nevertheless, Eisenberg et al. [2] succeeded in measuring reversal potentials under various salt concentration gradients and estimated the macroscopic ion-selectivity, i.e., the permeability ratios of Ca^{++}, Na^+ and K^+ to Cl^- were 0.3, 1.6 and 2.7, respectively. If the channel lifetime is prolonged, the reversal potential can be more easily measured at low peptide concentrations. Thus, as well as single-channel I–V_m measurements, use of tethered alamethicin would be of considerable benefit in determination of the reversal potential by macroscopic I–V_m measurements.

In a previous paper, we studied the effects of charged residues on the charge selectivity of alamethicin ion channels by comparing the single-channel conductance measured in solutions of K and Cl salts with bulky counterions. The results with alamethicin analogs with Glu7 (E7) instead of Gln7 (Q7) suggested that ionized E7 located at the narrowest part of the channel strongly enhanced cation-selectivity [21]. The charge selectivity of the channels, however, should be verified by measuring the reversal potentials. To measure the entire I–V_m relations of single channels, long lasting channels are required as above mentioned. Hence, we synthesized the alamethicin dimer (di-alm-Q7E18) N-terminally linked by a disulfide bond and succeeded to increase the open duration and to obtain the entire I–V_m relations of the single channels [30].

In this study, we synthesized a homodimer of an alamethicin analog with E7 (di-alm-E7Q18) by tethering alm-E7Q18 at the N-terminus by a disulfide bond. For di-alm-E7Q18 and di-alm-Q7E18 previously synthesized, the I–V_m relations and the reversal potentials were obtained at the single- and the multi-channel levels. The charge selectivity was determined from the reversal potential measured in asymmetric KCl solutions and the effects of ionized E7 and E18 on the charge selectivity were discussed.

2. Materials and methods

2.1. Peptide synthesis

The sequences of alamethicin Rf 30 (alm-Q7E18) and peptides used in this study are shown in Fig. 1. Alm-E7Q18 and di-alm-Q7E18 (a dimer of alm-Q7E18) were synthesized previously [21,30]. In this study, di-alm-E7Q18 was synthesized by the same method used for di-alm-Q7E18. Fig. 2 shows the ESI-MS chart of synthesized di-alm-E7Q18 (MW=4018.79) obtained using an API-3000K (PE Sciex), two peaks being found as: 2009.9 [M+2H$^+$] and 1340.4 [M+3H$^+$].

2.2. Channel current measurements

Currents through ion channels formed by peptides in diphytanoyl phosphatidylcholine bilayers were measured as described previously [21,30,32]. The bathing solutions (1 M and 3 M KCl) were buffered with either 10 mM MES–HCl (pH

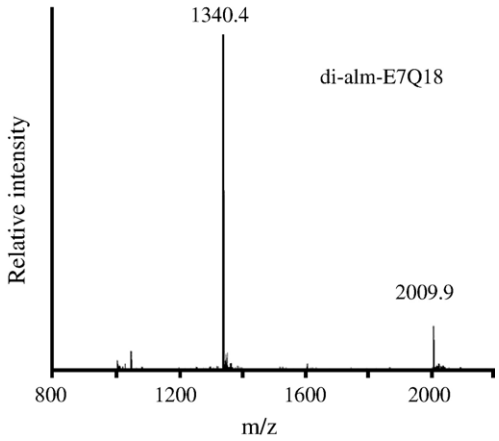

Fig. 2. EIS-MS chart of purified di-alm-E7Q18.

3.5) or 10 mM HEPES–KOH (pH 6.9–7.0). A pair of Ag–AgCl electrodes was used for current measurement and voltage supply. Peptides were added to one of the aqueous compartments (*cis*-side) to a final concentration of 1–5 nM for alm-E7Q18 and 0.1–2.5 nM for di-alm-E7Q18 and di-alm-Q7E18, and the other side (*trans*-side) is virtually grounded. Currents were measured using a home made current–voltage converter or an Axopatch 200B (Axon Instruments). Measurements were made at 25 ± 0.5 °C and the cut-off frequency was around 1 kHz. Single-channel recordings were made by applying a dc voltage of about 200 mV. For macroscopic current–voltage measurements, triangular wave voltages of 0.01 to 1 Hz (or the voltage sweep rate of 10–1000 mV/s) were applied to the membranes.

The current–voltage characteristics of the single channels of di-alm-Q7E18 and di-alm-E7Q18 were measured by applying a fast voltage ramp during the open states as described previously [30]. Briefly, when a single channel is formed under a dc voltage of ~200 mV, the voltage is linearly decreased to ~−200 mV and then is increased to ~200 mV at a sweep rate of 32 mV/ms. If the channel does not close during the voltage sweep, we can get the I–V_m curve after correction for the charging current of the membrane.

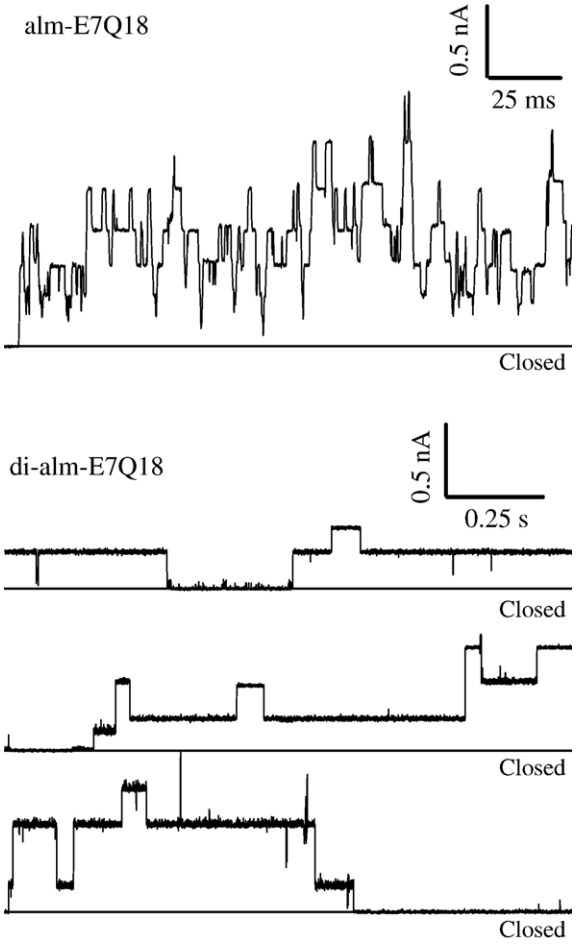

Fig. 3. Single channel recordings for alm-E7Q18 and di-alm-E7Q18 channels in 1 M KCl at pH6.7–6.9 and at 200 mV. Note the difference in time scale between alm-E7Q18 and di-alm-E7Q18. For di-alm-E7Q18, three traces are shown.

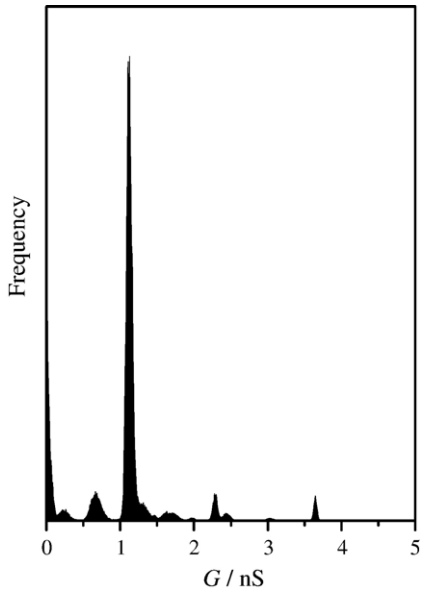

Fig. 4. Conductance histogram of di-alm-E7Q18 channels in 1 M KCl at pH 6.9.

2.3. Determination of charge selectivity

To determine the charge selectivity of channels, microscopic and macroscopic I–V_m curves were measured in asymmetric KCl solutions: c_c and c_t are KCl concentrations at the *cis*- and *trans*-sides, respectively. Since, with asymmetric KCl solutions,

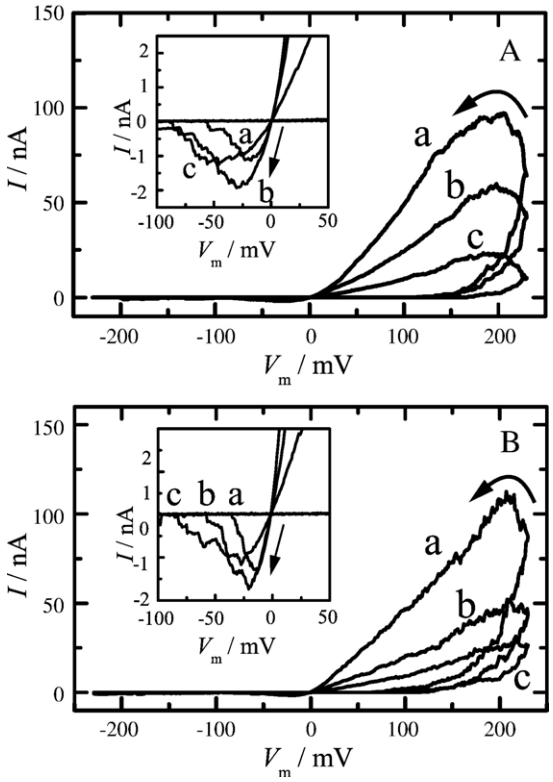

Fig. 5. Macroscopic I–V_m curves for (A) di-alm-Q7E18 and (B) di-alm-E7Q18 in 1 M KCl at pH 7.0. Sweep rates of voltage: in (A), (a) 46, (b) 92 and (c) 184 mV/s; in (B), (a) 92, (b) 184 and (c) 460 mV/s. Insets are closer looks of the negative slope conductance. Arrows indicate the directions of voltage sweep.

the applied voltage V is the sum of the electrode potential difference V_{el} and the membrane potential difference V_m, V_m was obtained by subtracting V_{el} from V as described previously [32].

When there is a difference between the permeability coefficients of K^+ and Cl^- denoted as P_K and P_{Cl}, the reversal potential E_m is evoked, which is represented by the Goldman–Hodgkin–Katz equation

$$E_m = \frac{RT}{F} \ln \frac{P_K a_t + P_{Cl} a_c}{P_K a_c + P_{Cl} a_t}, \quad (1)$$

where a_t and a_c are the activities of KCl solutions at the *trans*- and *cis*-sides, respectively.

3. Results and discussion

3.1. Single-channel recordings

Fig. 3 shows current fluctuations observed with lipid bilayers doped to alm-E7Q18 and di-alm-E7Q18 in 1 M KCl at pH 6.9 and at 200 mV. For alm-E7Q18, there appeared rapid transitions among several current levels as described in a previous paper [21]. This current behavior indicates that there are several channels of different conductance values because every current level is not a multiple of a unit current and that their lifetimes are less than 10 ms. In contrast to alm-E7Q18, di-alm-E7Q18 formed long lasting channels of a few conductance levels, indicating that particular channels are stabilized by tethering monomer peptides. Similar results were found for di-alm-Q7E18 as described previously [30]. The current traces for di-alm-E7Q18, however, were more noisy than those of di-alm-Q7E18 and various sublevels with slightly different conductance values were found. Fig. 4 shows one of the conductance histograms that were relatively often observed for di-alm-E7Q18. The main peak around 1.1 nS corresponds putatively to channels with six helices. The conductance value fluctuated among measurements, suggesting that the channels take several different conformations.

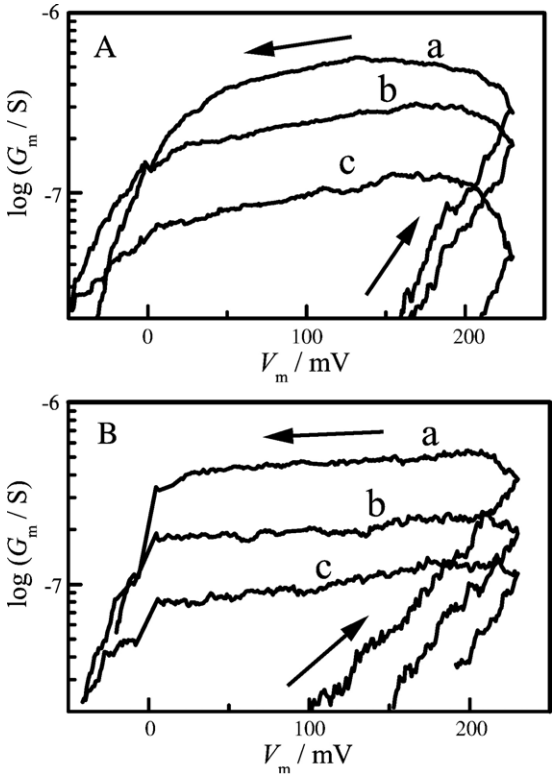

Fig. 6. Membrane conductance G_m plotted against membrane voltage V_m for (A) di-alm-Q7E18 and (B) di-alm-E7Q18 in 1 M KCl at pH 7.0. Data are the same as in Fig. 5. Arrows indicate the directions of voltage sweep.

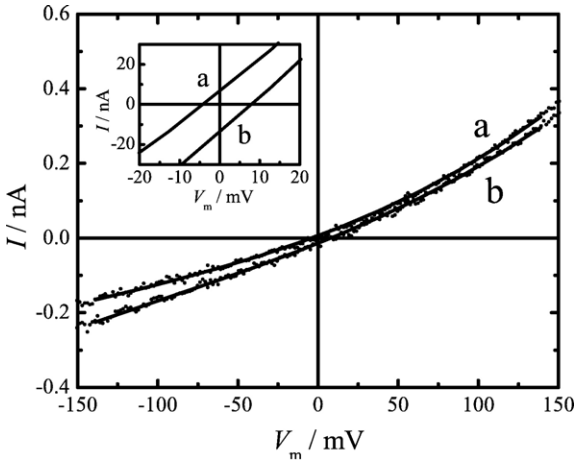

Fig. 7. Current–voltage (I–V_m) curves of di-alm-Q7E18 channels (putative hexameric channels) in asymmetric KCl solutions at pH 6.9. KCl solutions (*cis*/*trans*): 3 M/1 M for curve a and 1 M/3 M for curve b. Dots indicate the observed data. Solid curves were obtained by fitting a polynominal function to the data. Inset: a close look near the reversal potentials.

3.2. Macroscopic measurements

Fig. 5 shows macroscopic channel currents for di-alm-Q7E18 and di-alm-E7Q18 measured in 1 M KCl (pH 7.0) by varying voltage sweep rate. Channel currents were observed at

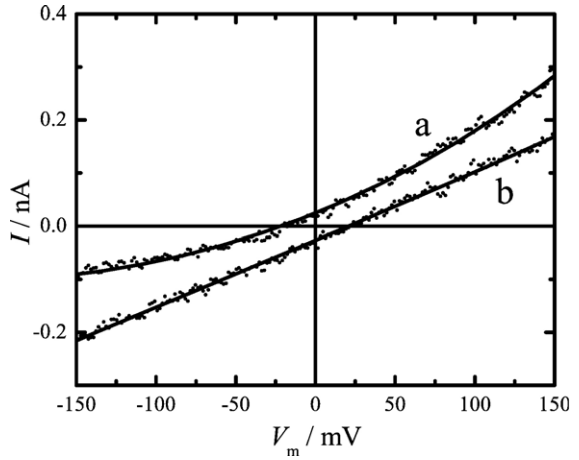

Fig. 8. Current–voltage (I–V_m) curves of di-alm-E7Q18 channels (putative hexameric channels) in asymmetric KCl solutions at pH 6.9. KCl solutions (*cis*/*trans*): 3 M/1 M for curve a and 1 M/3 M for curve b. Dots indicate the observed data. Solid curves were obtained by fitting a polynominal function to the data.

Table 1
Microscopic charge selectivity of di-alm-Q7E18 and di-alm-E7Q18 channels that are putative hexameric bundles

Peptides	P_K/P_{Cl}			
	KCl concentration (*cis*/*trans*)			
	1 M/3 M		3 M/1 M	
	pH 3.5	pH 7.0	pH 3.5	pH 7.0
Di-alm-Q7E18	1.4	1.8	1.3	1.2
Di-alm-E7Q18	1.3	38.9	1.2	8.5

The permeability ratios P_K/P_{Cl} were determined from the reversal potentials measured in asymmetric KCl solutions at 25 °C.

cis-positive voltages when peptides were added to the *cis*-side chamber, indicating peptides were N-terminally inserted in the membrane to form channels. The macroscopic current–voltage (I–V_m) relations traced wide hysteresis loops due to slow opening and closure of channels. At voltages below 0 mV, a negative slope conductance ($dI/dV_m<0$) appeared after a peak of negative current. Fig. 6 shows the logarithm of the cord conductance of membrane G_m ($G_m=I/V_m$) plotted against the membrane potential difference V_m. There were linear relations between log G_m and V_m in the ascending voltage limb and the slopes were almost independent of the voltage sweep rate. In the descending voltage limb, G_m gradually decreased after a broad peak but still remained high conductance levels even below 0 mV. Since G_m is proportional to the number of open channels, the results indicate that more than 100 channels are still open at 0 mV given the mean unit channel conductance is ~1 nS.

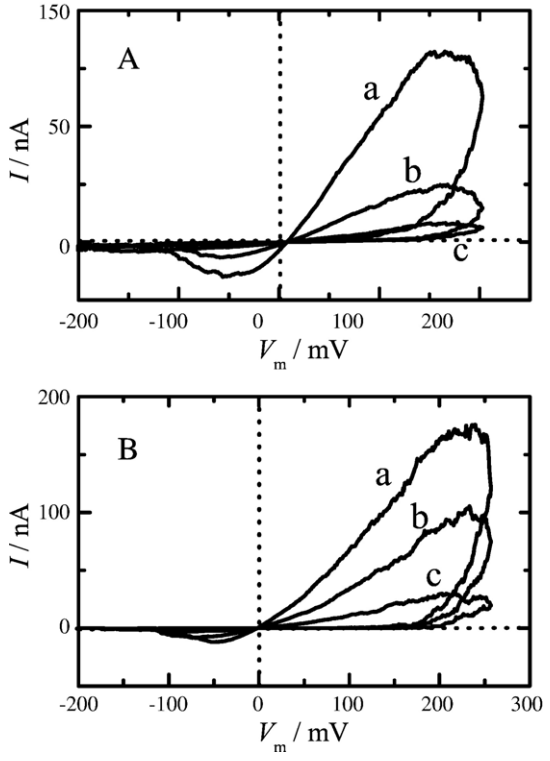

Fig. 9. Macroscopic I–V_m curves for di-alm-Q7E18 in asymmetric KCl solutions at pH 7.0. KCl solutions (*cis*/*trans*): (A) 1 M/3 M and (B) 3 M/1 M. Sweep rates of voltage: in (A), (a) 184, (b) 460 and (c) 920 mV/s; in (B), (a) 92, (b) 184 and (c) 460 mV/s.

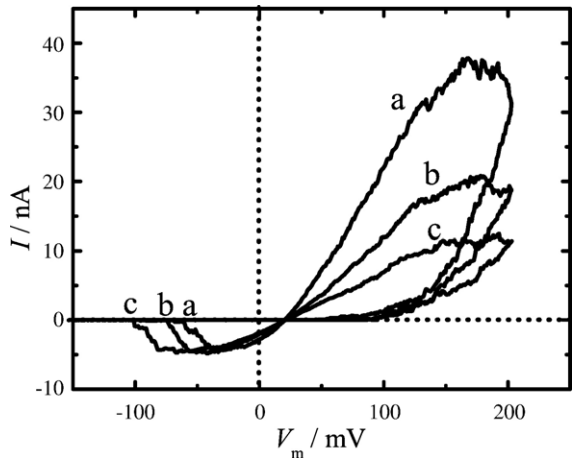

Fig. 10. Macroscopic I–V_m curves for di-alm-E7Q18 in 1 M/3 M KCl (*cis*/*trans*) at pH 7.0. Sweep rates of voltage: (a) 92, (b) 184 and (c) 460 mV/s.

Hence, we would expect that the reversal potential can be easily determined in the macroscopic I–V_m measurements with high voltage sweep rates for di-alm-Q7E18 and di-alm-E7Q18 in asymmetric salt solutions.

3.3. Current–voltage curves of single channels in asymmetric KCl solutions

The long open duration found in the single-channel recordings of di-alm-Q7E18 and di-alm-E7Q18 enables us to measure the entire current–voltage curves by applying a voltage

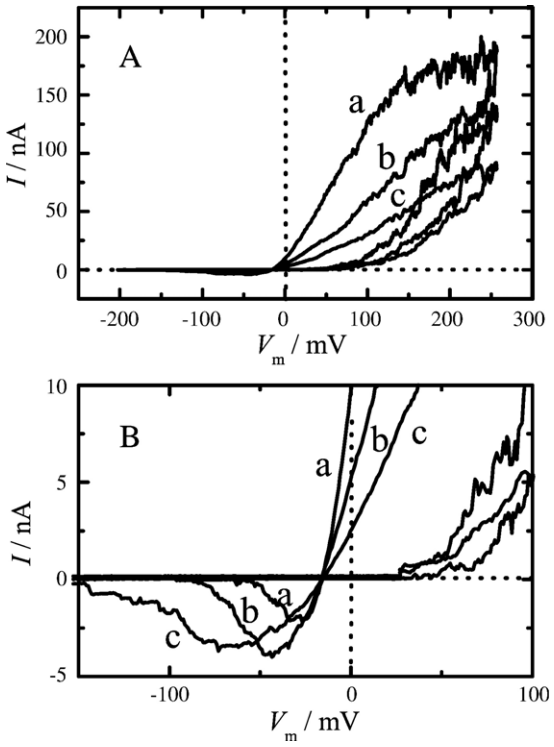

Fig. 11. Macroscopic I–V_m curves for di-alm-E7Q18 in 3 M/1 M KCl (*cis*/*trans*) at pH 7.0. (B) is a close look of (A) near the reversal potentials. Sweep rates of voltage: (a) 92, (b) 184 and (c) 460 mV/s.

ramp during the open state. Thus, we can obtain reversal potentials in asymmetric KCl solutions to determine the charge selectivity at the single-channel level. Fig. 7 shows the I–V_m curves for di-alm-Q7E18 at pH 6.9. The channels are putatively a bundle of six helices [30]. The reversal potentials were slightly negative (~−4 mV) for 3 M/1 M (*cis*/*trans*) KCl solutions, slightly positive (~8 mV) for 1 M/3 M KCl solutions, and were zero volt in symmetric KCl solutions (1 M and 3 M KCl). Fig. 8 shows the I–V_m curves of di-alm-E7Q18 channels with putatively hexameric helixes at pH 6.9. The reversal potentials were ~−22 mV (3 M/1 M) and ~26 mV (1 M/3 M), which were larger than those for di-alm-Q7E18.

The ratios of permeability coefficient P_K/P_{Cl} were calculated from the reversal potentials using Eq. (1), being summarized in Table 1. The di-alm-Q7E18 channels have moderate cation-selectivity at both pH 3.5 and pH 6.9. The ionization of E18 slightly enhanced cation-selectivity in 1 M/3 M but little did in 3 M/1 M. On the other hand, di-alm-E7Q18 channels showed strong cation-selectivity at pH 6.9 where E7 is ionized, whereas the charge selectivity at pH 3.5 was almost the same as that of di-alm-Q7E18. The charge selectivity for both di-alm-Q7E18 and di-alm-E7Q18 at pH 6.9 depended on the direction of KCl concentration gradient; the P_K/P_{Cl} for 1 M/3 M was higher than that for 3 M/ 1 M.

The values of P_K/P_{Cl} estimated for di-alm-Q7E18 and di-alm-E7Q18 were qualitatively consistent with those of the conductance ratio G_K/G_{Cl} measured for alm-Q7E18 and alm-E7Q18 channels using solutions of K and Cl salts with bulky organic counterions, i.e., $G_K/G_{Cl}=1.2$ for alm-Q7E18 and $G_K/G_{Cl}=4.2$ for alm-E7Q18 at pH 7.0 [21]. The conductance ratio, however, provided always lower values than the ratio of permeability coefficient as described by Starostin et al. [26].

3.4. Macroscopic I–V curves in asymmetric KCl solutions

Fig. 9 shows macroscopic I–V_m curves measured for di-alm-Q7E18 in asymmetric KCl solutions at pH 7.0. There found small reversal potentials as 8 mV for 1 M/3 M (*cis*/*trans*) and −3 mV for 3 M/1 M KCl. In contrast to di-alm-Q7E18, di-alm-E7Q18 showed much larger reversal potentials, i.e., 21 mV for 1 M/3 M KCl and −17 mV for 3 M/1 M KCl at pH 7.0 (Figs. 10 and 11). The reversal potentials indicated weak cation-selectivity for di-alm-Q7E18 and strong cation-selectivity for di-alm-E7Q18. The selectivity depended on the direction of KCl concentration gradient in a similar manner as described for the single channels in the previous subsection. Table 2 summarizes the macroscopic P_K/P_{Cl} calculated from the reversal potentials using Eq. (1). The P_K/P_{Cl} for di-alm-E7Q18 was much larger than that for di-alm-Q7E18 at pH 7.0, whereas almost the same P_K/P_{Cl} was obtained at pH 3.5 for the both peptides. This tendency was consistent with that obtained for the single channels (Table 1). The values of P_K/P_{Cl} were, however, smaller than those for the single channels of hexameric helixes. This is because there are channels that have larger pores than the hexameric channel in the macroscopic measurements. The ion-selectivity of the membrane is determined by the larger pores with smaller P_K/P_{Cl} values.

Table 2
Macroscopic charge selectivity of di-alm-Q7E18 and di-alm-E7Q18 channels

Peptides	P_K/P_{Cl}			
	KCl concentration (*cis*/*trans*)			
	1 M/3 M		3 M/1 M	
	pH 3.5	pH 7.0	pH 3.5	pH 7.0
Di-alm-Q7E18	1.3	1.8	1.2	1.3
Di-alm-E7Q18	1.3	5.5	1.1	4.4

The permeability ratios P_K/P_{Cl} were calculated from the reversal potentials measured in asymmetric KCl solutions at 25 °C.

3.5. Charge selectivity

We verified that the negatively charged E7 brings strong cation-selectivity and that the ionized E18 at the pore mouth little influences charge selectivity. This is reasonable because permeant ions receive strong electrostatic interactions from charged E7 at the narrowest part of the pore than charged E18 at the pore mouth. If the channels are of funnel shape as proposed by Fox and Richards [8], i.e., the C-terminal side has a wider mouth than the N-terminal one, little effect of ionized E18 on the charge selectivity is not surprising. However, this is not the case for the C-terminally linked alamethicin dimers, i.e., the replacement E18 by K18 converted weakly cation-selective channels to moderate anion-selective ones at neutral pH [26,28]. This could be because the residues at position 18 are closer each other for the C-terminally linked dimer than the N-terminally linked one.

The charge selectivity depended on the direction of KCl concentration gradient; P_K/P_{Cl} was 38.9 (1 M/3 M) and 8.5 (3 M/1 M) for channels of hexameric helices, and macroscopic P_K/P_{Cl} was 5.5 (1 M/3 M) and 4.4 (3 M/1 M). Although this is an interesting problem, here we only point out possible explanations. The permeability coefficient P is defined as $P=\beta D/d$, where β is the partition coefficient between the aqueous phase and the channel, D the diffusion constant of the ion within the channel and d the pore length. Since β and D relate to the free-energy profile in the pore, it is reasonable that the asymmetry of both of the channel structure and the electrostatic potential profile in the pore causes the asymmetry of the permeability coefficient. Further, since peptides are added to one side of the membrane, it is not ruled out that the surface potential at the membrane interface is modified by the adsorbed peptides to result in the asymmetry of the surface potentials.

Acknowledgements

We thank Dr. Kenich Morigaki for his critical reading of this manuscript and helpful discussion.

References

[1] P. Mueller, D.O. Rudin, Action potentials induced in biomolecular lipid membranes, Nature 217 (1968) 713–719.
[2] M. Eisenberg, J.E. Hall, C.A. Mead, The nature of the voltage-dependent conductance induced by alamethicin in black lipid membranes, J. Membr. Biol. 14 (1973) 143–176.

[3] L.G.M. Gordon, D.A. Haydon, Potential-dependent conductances in lipid membrane containing alamethicin, Philos. Trans. R. Soc. Lond., B 270 (1975) 433–447.
[4] R.J. Cherry, D. Chapman, D.E. Graham, Studies of the conductance changes induced in bimolecular lipid membranes by alamethicin, J. Membr. Biol. 7 (1972) 325–344.
[5] L.G.M. Gordon, D.A. Haydon, The unit conductance channel of alamethicin, Biochim. Biophys. Acta 255 (1972) 1014–1018.
[6] G. Boheim, Statistical analysis of alamethicin channels in black lipid membranes, J. Membr. Biol. 19 (1974) 277–303.
[7] C. Baumann, P.J. Mueller, A molecular model of membrane excitability, J. Supramol. Struct. 2 (1974) 538–557.
[8] R.O. Fox, F.M. Richards, A voltage-gated ion channel model inferred from the crystal structure of alamethicin at 1.5-A resolution, Nature 300 (1982) 325–330.
[9] R. Latorre, O. Alvarez, Voltage-dependent channels in planar lipid bilayer membranes, Physiol. Rev. 61 (1981) 77–150.
[10] M.S.P. Sansom, The biophysics of peptide models of ion channels, Prog. Biophys. Mol. Biol. 55 (1991) 139–235.
[11] G.A. Woolley, B.A. Wallace, Model ion channels: gramicidin and alamethicin, J. Membr. Biol. 129 (1992) 109–136.
[12] D.S. Cafiso, Alamethicin: a peptide model for voltage gating and protein–membrane interactions, Annu. Rev. Biophys. Biomol. Struct. 23 (1994) 141–165.
[13] H. Duchlohier, H. Wróblewski, Voltage-dependent pore formation and antimicrobial activity by alamethicin and analogues, J. Membr. Biol. 184 (2001) 1–12.
[14] J.E. Hall, I. Vodyanoy, T.M. Balasubramanian, G.R. Marshall, Alamethicin, a rich model for channel behavior, Biophys. J. 45 (1984) 233–247.
[15] G. Molle, H. Duclohier, S. Julien, G. Spach, Synthetic analogues of alamethicin: effect of C-terminal residue substitutions and chain length on the ion channel lifetimes, Biochim. Biophys. Acta 1064 (1991) 365–369.
[16] H. Duclohier, G. Molle, J.Y. Dugast, G. Spach, Prolines are not essential residues in the "barrel-stave" model for ion channels induced by alamethicin analogues, Biophys. J. 63 (1992) 868–873.
[17] G. Molle, J.Y. Dugast, G. Spach, H. Duclohier, Ion channel stabilization of synthetic alamethicin analogs by rings of inter-helix H-bonds, Biophys. J. 70 (1996) 1669–1675.
[18] C. Kaduk, H. Duclohier, M. Dathe, H. Wenschuh, M. Beyermann, G. Molle, M. Bienert, Influence of proline position upon the ion channel activity of alamethicin, Biophys. J. 72 (1997) 2151–2159.
[19] C. Kaduk, M. Dathe, M. Bienert, Functional modifications of alamethicin ion channels by substitution of glutamine 7, glycine 11 and proline 14, Biochim. Biophys. Acta 1373 (1998) 137–146.
[20] J. Jacob, H. Duclohier, D.S. Cafiso, The role of proline and glycine in determining the backbone flexibility of a channel-forming peptides, Biophys. J. 76 (1999) 1367–1376.
[21] K. Asami, T. Okazaki, Y. Nagai, Y. Nagaoka, Modification of alamethicin ion channels by substitution of Glu-7 for Gln-7, Biophys. J. 83 (2002) 219–228.
[22] S. You, S. Peng, L. Lien, J. Breed, M.S.P. Sansom, G.A. Woolley, Engineering stabilized ion channels: covalent dimers of alamethicin, Biochemistry 35 (1996) 6225–6232.
[23] A. Matsubara, K. Asami, A. Akagi, N. Nishino, Ion-channels of cyclic template-assembled alamethicins that emulate the pore structure predicted by the barrel-stave model, Chem. Commun. (1996) 2069–2070.
[24] D.C.J. Jaikaran, P.C. Biggin, H. Wenschuh, M.S.P. Sansom, G.A. Woolley, Structure–function relationships in helix-bundle channels probed via total chemical synthesis of alamethicin dimers: effects of a Gln7 to Asn7 mutation, Biochemistry 36 (1997) 13873–13881.
[25] G.A. Woolley, P.C. Biggin, A. Schultz, L. Lien, D.C.J. Jaikaran, J. Breed, K. Crowhurst, M.S.P. Sansom, Intrinsic rectification of ion flux in alamethicin channels: studies with an alamethicin dimer, Biophys. J. 73 (1997) 770–778.
[26] A.V. Starostin, R. Butan, V. Borisenko, D.A. James, H. Wenschuh, M.S.P. Sansom, G.A. Woolley, An anion-selective analogue of the channel-forming peptide alamethicin, Biochemistry 38 (1999) 6144–6150.
[27] H. Duclohier, K. Kociolek, M. Stasiak, M.T. Leplawy, G.R. Marshall, C-terminally shortened alamethicin on templates: influence of the linkers on conductances, Biochim. Biophys. Acta 1420 (1999) 14–22.
[28] V. Borisenko, M.S.P. Sansom, G.A. Woolley, Protonation of lysine residues inverts cation/anion selectivity in a model channel, Biophys. J. 78 (2000) 1335–1348.
[29] S. Futaki, M. Fukuda, M. Omote, K. Yamauchi, T. Yagami, M. Niwa, Y. Sugiura, Alamethicin–leucine zipper hybrid peptide: a prototype for the design of artificial receptors and ion channels, J. Am. Chem. Soc. 123 (2001) 12127–12134.
[30] T. Okazaki, M. Sakoh, Y. Nagaoka, K. Asami, Ion channels of alamethicin dimer N-terminally linked by disulfide bond, Biophys. J. 85 (2003) 267–273.
[31] W. Hanke, G. Boheim, The lowest conductance state of the alamethicin pore, Biochim. Biophys. Acta 596 (1980) 456–462.
[32] N. Koide, K. Asami, T. Fujita, Ion-channels formed by hypelcins, antibiotic peptides, in planar bilayer lipid membranes, Biochim. Biophys. Acta 1326 (1997) 47–53.